# Dual-Polarized Wide-Angle Scanning Phased Array Antenna for 5G Communication Systems

Yang, Guangwei; Zhang, Shuai

*Published in:*
I E E E Transactions on Antennas and Propagation

*DOI (link to publication from Publisher):*
10.1109/TAP.2022.3141188



*Publication date:*
2022

*Document Version*
Accepted author manuscript, peer reviewed version



*Citation for published version (APA):*
Yang, G., & Zhang, S. (2022). Dual-Polarized Wide-Angle Scanning Phased Array Antenna for 5G Communication Systems. *I E E E Transactions on Antennas and Propagation*, *70*(9), 7427-7438. Advance online publication. https://doi.org/10.1109/TAP.2022.3141188

# Dual Polarized Wide-Angle Scanning Phased Array Antenna for 5G Communication System

Guangwei Yang, *Member, IEEE,* and Shuai Zhang, *Senior Member, IEEE*

*Abstract*—**A dual-polarized phased array antenna is presented with wide-angle scanning capability in this paper. To improve the mutual coupling in the array, a current cancellation method (CCM) is proposed by changing the current distribution on the excited unit to induce a pair of the canceled currents on the adjacent unit. Meanwhile, this current distribution broadens the beam-width of the unit in the array. Besides, the proposed method can also optimize the array unit size and achieve a small inter-unit distance for wide-angle scanning capability. A low-profile dual-polarization antenna operating in the bandwidth from 4.4 GHz to 5.0 GHz is designed as a linear array and a planar array to verify the proposed method. Regardless of the linear array or planar array, the mutual coupling in the array is below -19 dB, which is better than that in conventional arrays. Meanwhile, the antenna unit in the array can radiate a wide-beam pattern. Two arrays can scan over ±60° for both polarizations. Within the scanning range, the realized gain reduction is less than 3 dB and the side-lobe level is lower than -7.5 dB. To verify the performance, two array antenna prototypes are fabricated and tested. The experimental results agree well with the simulation.**

***Index Terms*—wide-beam, dual-polarized antenna, decoupling, phased array antennas, wide-angle scanning, current cancellation.**

## I. Introduction

IN recent years, wide-angle scanning technology has a rapid development, which has been applied into phased arrays for many fields to solve the large coverage issues of the array with high gain. However, for satellite communications, fifth-generation (5G) communication systems, Synthetic Aperture Radars (SAR), and so on, the array antenna not only needs to realize wide-angle scanning performance but also has a dual-polarized function. Because the dual-polarized capability can extend the system capacity without increasing the size, and implement polarization diversity technology to achieve multipath fading resistance. To obtain the above two functions, not only the wide beam of the antenna element must be designed, but also the decoupling in the array and port isolation need to be solved. Besides, some other factors such as profile and cost must also be considered. Therefore, this is a complex and urgent issue, which needs to be solved by global scholars.

For the wide-angle scanning phased array antenna, there are some methods to improve: a) The far-field of the array antenna is equal to an antenna element pattern multiplied by the array factor, under ideal conditions. Hence, it is a good measure to improve the wide-angle scanning performance of the array by extending the beam-width of the antenna element. The beam-width of the antenna element is extended to more than 100° in two planes by the metal-cavity structure, which makes the beam of the array scan from -60° to +60° [1]. The special structure with the metal via is an excellent method to improve the beam-width of the element to enhance the wide-angle scanning capability of the array [2]. Besides, adding the metal walls on both sides of the patch [3], designing the tapered slot [4], utilizing the substrate integrated waveguide (SIW)-slot technology to reduce the size of the element [5], and so on, can broaden the beam-width of the element in the limited space. b) As we know, the array inter-element space needs to be compact if the beam of the array should scan for large coverage. However, the strong mutual coupling in the array can be produced by the compact array inter-element space. It would affect the pattern of the element in the array, which seriously reduces the scanning range and even leads to scanning blindness in limited space. Some methods have applied to solve this problem such as adding the dielectric sheet in front of the array [6], adding multilayer substrates on the metal ground [7], using a dielectric layer with a metal sheet like a patch antenna-like structure [8], changing the ground plane to the defected ground structure (DGS) [9], electromagnetic bandgap (EBG) structure [10], and high impedance surfaces (HIS) [11] [12], using the feed network to decoupling [13] [14], designing the metal-cavity like SIW [15] and substrate-integrated cavity-backed (SICB) structure [16]. These techniques can eliminate surface waves and mutual coupling in the array for improving the wide-angle scanning performance. Although the above methods have achieved some improvement for the wide-angle scanning capability of linear or planar array antennas, at present, there is almost no simple and effective method that can simultaneously improve the coupling of the array and broaden the beam-width to achieve excellent wide-angle scanning characteristics.

For some fields like satellite communications and 5G communication systems, a single-polarization manner is difficult to satisfy the communication requirements. And the dual-polarization manner has been used in the above fields. There are the following antenna types to investigate for the dual-polarization like: dipole antenna [17-19], microstrip antennas [20-22], magneto-electric (ME) dipole antennas [23-25], dielectric resonator antennas [26-28]. These antennas have many advantages such as low-cross polarization, low forward/backward (F/B) radiation ratio, and wide frequency band. However, a compact and low-profile, low-cost,

Manuscript received Mar. 20, 2021. This work has been supported by AAU Young Talent Program and the UK Royal Society Newton International Fellowship under Grant NIF/R1/191365. (Corresponding author: *Shuai Zhang*)

The authors are with the Antennas, Propagation and Millimeter-Wave Systems Section, Department of Electronic Systems, Aalborg University, 9220 Aalborg, Denmark. (E-mail gwyang086@gmail.com; sz@es,aau.dk).

Guangwei Yang is also with the School of Electronic Engineering and Computer Science, Queen Mary University of London, London E1 4NS, UK.

lightweight dual-polarized antenna with a wide beam has rarely been realized by now.

It is an indisputable fact that the dual-polarization wide-angle scanning planar phased array will be a pivotal enabling technology in the 5G communication systems. In recent years, the dual-polarized wide-angle scanning antenna has gotten some achievements based on the above dual-polarized antenna elements [29-36]. The HIS is applied to substitute the ground plane for realizing low profile dual-polarized antenna, where can scan ±50° for each polarization in a wide frequency band [29]. The zeroth-order resonance and $TM_{01}$ mode resonance are generated in the mushroom-shaped patch to broaden the beam-width of the dual-polarized microstrip antenna for wide-angle scanning performance [30]. The dual-polarized patch antenna with vertical orthogonal baluns and cavity-backed structure is designed to realize scan ±45° in H- and E-planes for either polarization [31]. A dual-polarized aperture-stacked patch antenna is applied to achieve the wide-angle scanning ability for reflectarrays [32]. A multimode patch antenna is applied to improve dual-polarized wide-angle scanning ability [33]. However, Due to the complexity of the structure, the high cost, and the limited scanning capability, it cannot meet the current relatively high application requirements for the proposed communication systems. Besides, some dual-polarization connected-dipole arrays based on tightly coupled technology are presented in [34]-[36] to improve wide-angle scanning performance. But the tightly coupled array or connected array is not suitable for 5G communication systems (e.g., MIMO) since the interelement mutual coupling is required to be low when each array element works in an active or passive mode independently. Overall, to successfully apply this new technology for future commercial applications, many scholars around the world have conducted in-depth research on the actual implementation of this technology from both theoretical and practical perspectives.

To confront these issues, a new method named the current cancellation method (CCM), is proposed, investigated, and demonstrated to achieve wide-angle scanning capability for a dual-polarized array antenna in this paper. This method can improve the mutual coupling in the array by obtaining the canceled induced currents on each neighboring unit cell of the array. Meanwhile, the beam-width of the unit in the array can be broadened by this method. Besides, by bending the patch of the unit, the compact antenna structure is realized. To this end, a new and simple dual-polarization antenna array is designed to realize the proposed method. The antenna unit has a simple and compact structure and is comprised of two metal feed lines, a pair of regular shaped metal plates, the ground plane, and a dielectric substrate. A dual-polarized one-by-eight linear array and a dual-polarized four-by-eight planar array based on this antenna unit are designed and fabricated to verify the CCM for wide-angle scanning capability. The measured results reveal that the mutual coupling between the adjacent units is better than -19 dB with smaller than 0.5λ inter-element space for two polarizations regardless of the linear array or planar array in the bandwidth of 4.4 -5.0 GHz (n79 of 5G NR frequency bands). Meanwhile, the wide beam unit is realized in the linear and planar arrays. Two type arrays can all scan the coverage of ±60° in *x*-polarization and ±65° in the *y*-polarization with the lower realized gain reduction and low side-lobe level, respectively. For the four-by-eight planar array, the above wide-angle scanning capability is also realized. Hence, the wide-angle scanning capability is validated in the dual-polarized planar phased array. Through the above description, the novelties of this work are as follows:

(a) A simple method is presented to improve the mutual coupling in the array and broaden the beam-width for wide-angle scanning capability, simultaneously.
(b) A compact and low-profile dual-polarization antenna with wide beam-width, simple structure, and low cost is designed in this paper.
(c) A simple and good wide-angle scanning dual-polarized planar array is studied, which can scan over ±60° for both polarizations with the lower realized gain reduction and low side-lobe level, respectively.

The organization of the paper is as follows. In Section II, the proposed design approach is analyzed. In Section III, A 1 to 8 linear dual-polarized array is designed to illustrate the dual-polarized wide-angle scanning performance by wide-beam units and the decoupling technology. The planar array is studied, and its scanning performance is verified in Section IV. The dual-polarized wide-angle scanning phased array works are discussed in Section V. Finally, a summary together with concluding remarks is given.

## II. Design Approach and Analysis

For wide-angle scanning performance of the phased array antenna, in general, the following three aspects need attention: a) the coupling among array units that could lead to the scanning blindness, b) the wide beam performance of the array unit to ensure the lower gain reduction at the large scanning coverage, and c) the small inter-unit space to minimize the possibility of grating lobes. In this paper, a simple and efficient approach is presented to solve the above issues, simultaneously.

### *A. Decoupling principle*

To clearly illustrate the decoupling principle, two referenced arrays are presented for comparison with the proposed array. The inter-unit spacing of three arrays and the dimensions of the array units are kept the same. Besides, one of the units is excited and the other units are terminated with the matching load. As shown in Fig. 1, the schematic diagram for the E-plane array is depicted. A traditional microstrip array with its current distribution is given in Fig. 1(a), as all we know, the excited unit can produce the horizontal current on the patch, which could induce an opposite and strong horizontal current on the patch of the adjacent matching unit because of the unit-spacing. So the mutual coupling in the proposed array is intensity. In Fig. 1(b), a pair of the bended plates are applied for the array to produce the horizontal and vertical currents on the antenna unit. It is the same to the Ant. a, the horizontal current can induce the horizontal current with opposite direction on the matching unit.

Since the adjacent vertical plates are relatively close, the vertical current on the matching unit is induced from the vertical current on the excited unit and it is opposite to the vertical current on the excited unit. Because of this vertical current, two induced currents are canceled on the matching unit. Hence, a field of the current cancellation is obtained, and the mutual coupling in the array is weakened. But the canceling currents are a little weak because the induced vertical current is relatively weak. To improve the proposed decoupling performance, the vertical parts of the adjacent units are connected by metal sheets, which are shown in Fig. 1(c). The vertical currents on the excited unit are stronger, so that the vertical current on the matching unit is also strengthened, which leads to a better induced current cancellation on the matching unit. Therefore, a good decoupling for the E-plane array is realized by the proposed method. Note that the proposed method is different from the neutralization line [37][38], which would produce a neutralized field by using a line to connect the adjacent antenna units. Furthermore, the neutralization line mode [37][38] is very difficult to excite in a large array. Meanwhile, the proposed approach doesn't require the addition of other redundant structures, such as metal strips [39], and the application of complex feed networks [40] [41] to reduce coupling between arrays, and more importantly, our design can be applied to achieve excellent decoupling in compact structures of dual-polarized array antennas.

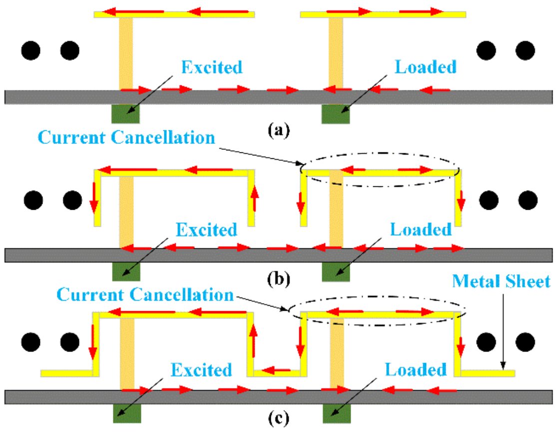


Fig. 1. Decoupling principle in E-plane: (a) Ant. a; (b) Ant. b; (c) Ant. c.

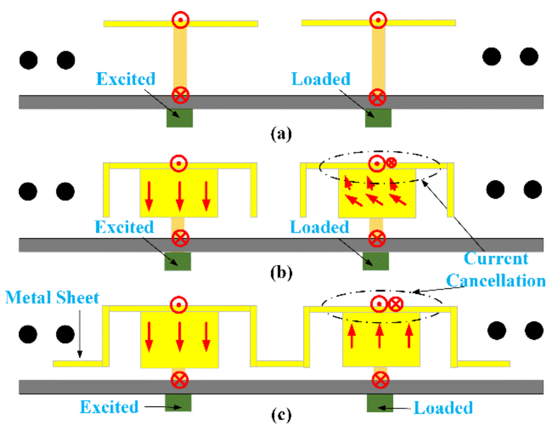


Fig. 2. Decoupling principle in H-plane: (a) Ant. a; (b) Ant. b; (c) Ant. c.

Similarly, the proposed method also is used to improve the mutual coupling in an H-plane array. As shown in Fig. 2, when the excited unit produces the horizontal current, the adjacent matching unit is induced the same horizontal current, which is the classical induced mode in the array antenna. As given in Fig. 2(b), the vertical part is formed by bending the patch, which is the same as the one in Fig. 1 (b). Hence, the vertical current is produced on the vertical part of the patch, which can induce a vertical current on the vertical plate of the matching unit. This can lead to producing the current cancellation on the patch. But it is a little weak since the induced vertical current on the matching unit is not very well. To enhance the current cancellation, the metal sheet is applied to the proposed array as shown in Fig. 2(c). The induced vertical current on the matching unit is strengthened and a better current cancellation also is realized on the matching unit in the array. Therefore, a good decoupling for the H-plane array is also achieved by the proposed method.

### *B. Broadening beam-width principle*

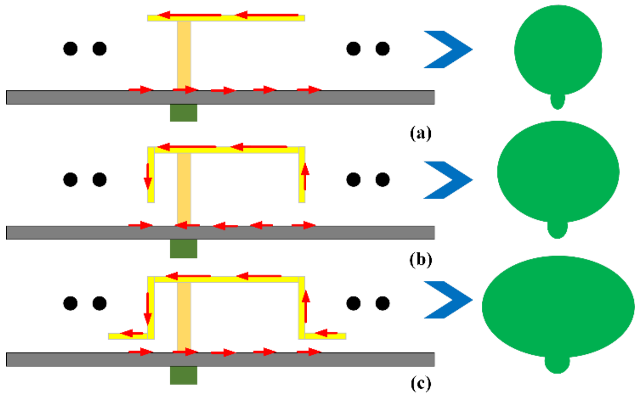


Fig. 3. Broadening beam-width principle: (a) Ant. a; (b) Ant. b; (c) Ant. c.

The proposed method could not only improve the mutual coupling in the array but also broaden the beam-width of the unit in the array. As depicted in Fig. 3, for Ant. a, it just produces the horizontal current, which is similar to the patch antenna, and radiates a broadside pattern. When a part of the horizontal plate is bent to form a vertical plate, as shown in Fig. 3(b). The vertical and horizontal currents are produced on the Ant. b. Hence, the radiation pattern is broadened [42], but the beam-width is not good enough. To obtain a wider radiation pattern, the vertical current should be enhanced. The connecting metal sheet could solve this problem. From Fig. 3 (c), the strengthened vertical current could be obtained to guarantee the proposed antenna to radiate with a wide beam.

## III. DUAL-POLARIZED LINEAR ARRAY

### *A. Array antenna unit design*

Based on the principle from the above section, a dual-polarized antenna unit is designed as shown in Fig. 4, which depicts the evolution structure in three steps. Ref. a is a dual-polarized patch antenna, which is similar to the Ant. a. Then the plates are bent to form the vertical plate, as shown in Fig. 4(b). Ultimately, the metal sheet is added in Ref. b, the proposed dual-polarized antenna is designed, which is a compact and simple structure. The detailed configuration is given in Fig. 5, which is a simple metal structure and consists of a metal ground plane, four bent metal plates with four circular slots, four metal sheets, and two L-shaped feed lines. The metal sheet is printed on the substrate (which is the poly-tetra propylene (PP) with a relative dielectric constant of 2.2 and a loss tangent of 0.002, and the thickness ($h_3$) is 1 mm). Note that the proposed design is a new dual-polarized antenna which has a novel structure for wideband and wide beam characteristics and doesn't the balun-fed structure in comparison with the traditional (planar) dipole antennas [43]-[45]. Besides, the profile of the antenna is low and 7.0 mm, which is about 0.12λ (at 5.0 GHz). The parameters of the proposed dual-polarized antenna unit are shown in Table I.

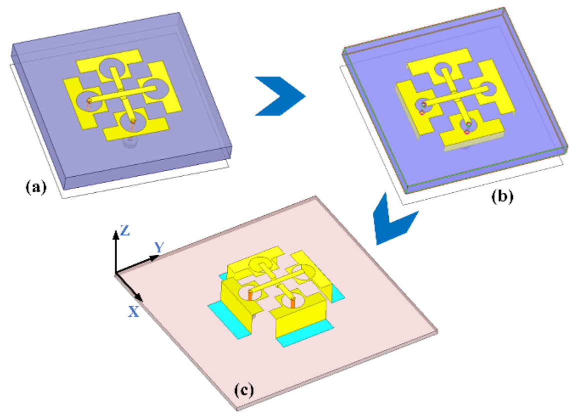


Fig. 4. Steps to realize the proposed antenna unit based on the above principles: (a) Ref. a; (b) Ref. b; (c) Pro.

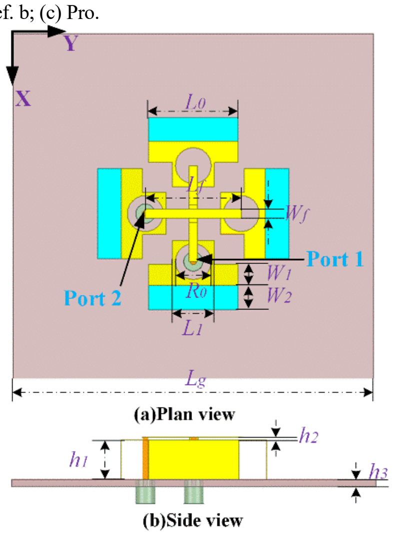


Fig. 5. Configuration of the proposed antenna unit: (a) Plan view; (b) Side view.

TABLE I
DIMENSIONS OF THE WIDE-BEAM AND DUAL-POLARIZATION ANTENNA

| Parameter | $L_g$ | $L_0$ | $L_1$ | $L_f$ | $W_1$ | $W_2$ | $W_f$ | $r_0$ | $h_1$ | $h_2$ |
|---|---|---|---|---|---|---|---|---|---|---|
| Units (mm) | 60 | 15.5 | 7.5 | 18 | 3.5 | 4 | 1.5 | 3 | 6.5 | 0.5 |

To verify the design approach, the *S*-parameters and radiation patterns of the three antennas are reported in Fig. 6(a) and Fig. 7, respectively. From Ref. a to Pro., we can find that these antennas operate in the same frequency band, and the impedance matching changes better to lead to a wide operating frequency band. And the port isolation of the antenna is also improved and up to around 30 dB. For the radiation pattern, as indicated by the broadening beam-width principle, the beam-width in two planes of Ref. b is broadened because of producing the vertical current. A wider radiation pattern is realized by the proposed antenna because of optimizing the strength of the vertical current. Meanwhile, several substrates with different thicknesses are applied to ensure that three type antenna units have the same dimensions for better analysis of the proposed decoupling principle. Ref. a has a thicker substrate, and Ref. b has a thin substrate. The proposed one doesn't have the substrate. Hence, by adding the connecting metal sheet, the proposed method can be beneficial to reduce the antenna size. Additionally, the comparisons with the three antennas are given in Table II. Note that the size and beamwidth of the proposed antenna are improved without sacrificing the operating bandwidth, radiation efficiency, etc. Also, the input impedance of three antennas is shown in Fig. 6(b), which indicates the design variation how to improve the resonance mode of the antenna to show the proposed design merit.

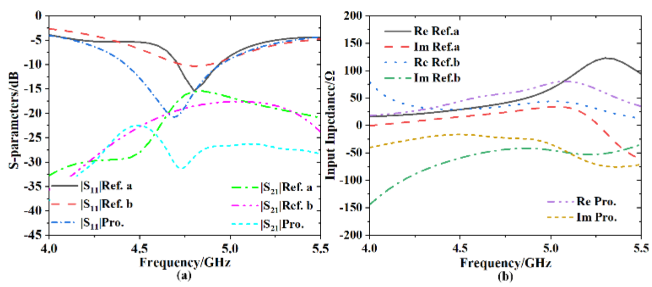


Fig.6. (a) *S*-parameters and (b) input impedance of three antenna units.

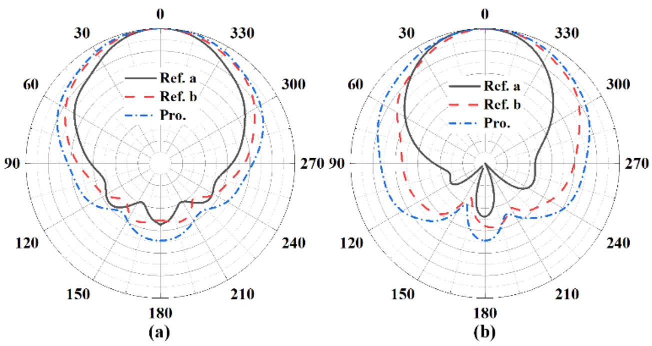


Fig. 7. Normalized radiation patterns of three antenna units at each resonance frequencies of port 2 in (a) *xoz*-plane; (b) *yoz*-plane.

TABLE II
COMPARISON OF THE REFERENCE ANTENNAS WITH THE PROPOSED ANTENNA

| Ref. | BW | Gain(dBi) | HPBW (*xoz*-pl.) | HPBW (*yoz*-pl.) | RE |
|---|---|---|---|---|---|
| a | 4.2% | 7.3 | 58° | 58° | 78.7% |
| b | 3.1% | 6.8 | 83° | 69° | 86.1% |
| Pro. | 12.8% | 5.4 | 102° | 102° | 87.1% |

BW: bandwidth; HPBW: half-power beamwidth; RE: radiation efficiency

## *B. One-by-eight dual-polarized linear array antenna*

As shown in Fig. 8, the 1 × 8 linear array with the metal sheet is presented and analyzed, which has a suitable unit-spacing (30 mm or 0.5λ at 5.0 GHz) for large scanning coverage. The array comprises eight antenna units that are connected by the metal sheet. A dielectric substrate is used to print the metal sheet, which has the same size as the ground plane of 60 mm×300 mm. Some small PP dielectric strips are used to ensure that the feed line is placed horizontally above the patch. The proposed antenna has a 3-D structure with a low-cost metallic design, which is easy to fabricate and implement by mechanical processing. The proposed antenna can also be revised with planar multilayer due to its simple configuration.

To verify the effectiveness of the proposed method, simulations of three type arrays are carried out with CST Microwave Studio. The simulated S-parameters of the array are shown in Fig. 9. The operating frequency band of the array is from 4.35 to 5.15 GHz in *x*-polarization and 4.4 to 5.05 GHz in *y*-polarization, respectively. Because of the proposed method, the port-to-port mutual coupling of the array in two polarizations is all better than -20 dB in the whole operating frequency band and even up to -25 dB in some frequencies. The isolation of the dual-polarized ports in each unit in the array is also better than 20 dB.

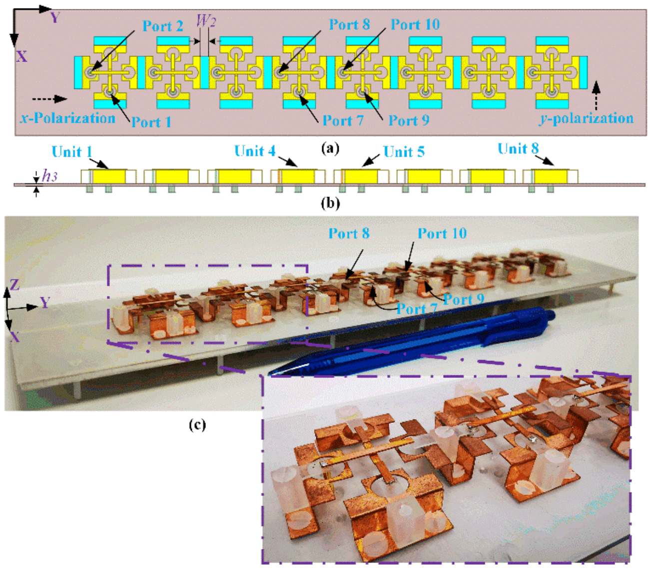


Fig. 8. Geometry and prototype of one-by-eight dual-polarized linear array antenna.

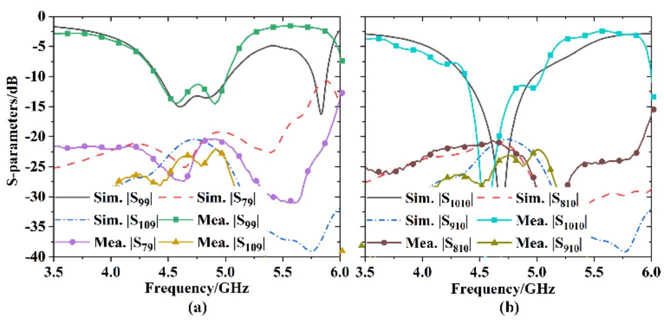


Fig. 9. Simulated and measured S-parameters of the units in the dual-polarization linear array: (a) *x*-polarization; (b) *y*-polarization.

Ref. a and Ref. b are also designed to one-by-eight linear arrays for simulations, respectively, compared with the proposed array. As shown in Fig. 10, the mutual coupling in each array is reported. In the operating frequency band, it is found that the mutual coupling of the array is improved for two polarizations, which is consistent with the principle in Section II-A. As the horizontal plate is bent and the metal sheet is added, the mutual coupling in the array gradually is improved, especially in the proposed array which is better than -20 dB in two planes. The radiation patterns of the unit in three arrays are given in Fig. 11. The proposed method could also broaden the beam-width of the pattern in the array. Meanwhile, the curve of the pattern is relatively smooth without depression, which is because of the better mutual coupling in the array. Besides, the measured results are similar to the simulated ones. Therefore, the proposed method is also used to broaden the beam-width of the unit in the array.

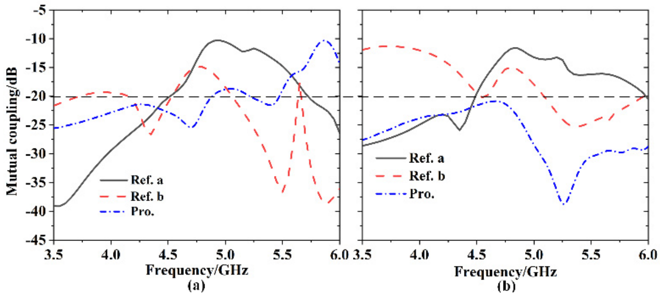


Fig. 10. Port-to-port mutual coupling of three type antenna arrays: (a) *x*-polarization; (b) *y*-polarization.

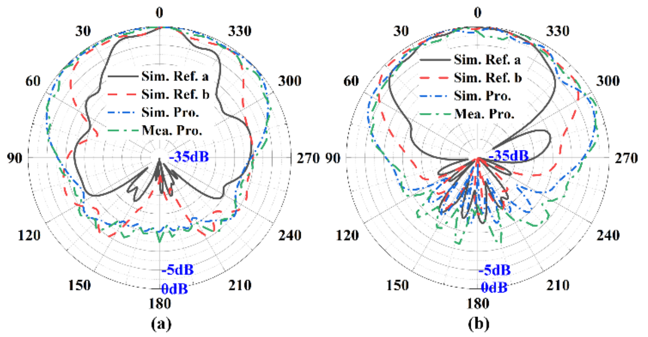


Fig. 11. Radiation patterns of the units in three linear arrays in *yoz*-plane: (a) port 7; (b) port 8.

For detailed validation of the proposed method in the linear array, the simulated current distributions of the three type arrays are analyzed in Fig. 12 and Fig. 13. It can be seen that the current distribution in three arrays is the same as the analysis in Section II-A. In Fig. 12, with the varying structure of the antenna, the vertical current is produced on the excited unit and induces the vertical current on the adjacent unit to lead to obtaining the current cancellation field on the adjacent unit in the array, which is similar to the one in Fig. 1 (b). Meanwhile, In Fig. 12 (c), the metal sheet is applied to enhance the vertical current, and the strengthened opposite horizontal current is produced. Hence, the better current cancellation on the adjacent unit is obtained by comparing it with the one in Fig. 12 (b). In Fig. 13, similarly, the current cancellation is also obtained in the H-plane array. Because the bent plate can produce a vertical current on the excited unit, the induced vertical current on the adjacent unit changes the current distribution on the patch. And the better current cancellation is obtained on the adjacent unit since the strong opposite current is produced by the metal sheet as shown in Fig. 13 (c). Therefore, the mutual coupling in the proposed dual-polarized array is improved by the proposed method.

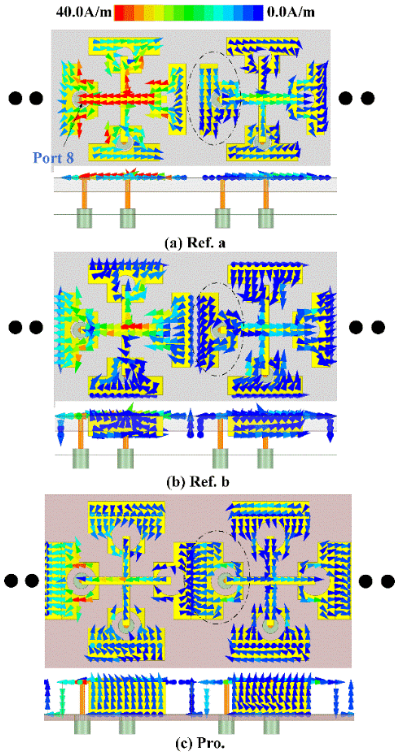


Fig. 12. Current distribution of three antenna arrays with exciting port 8.

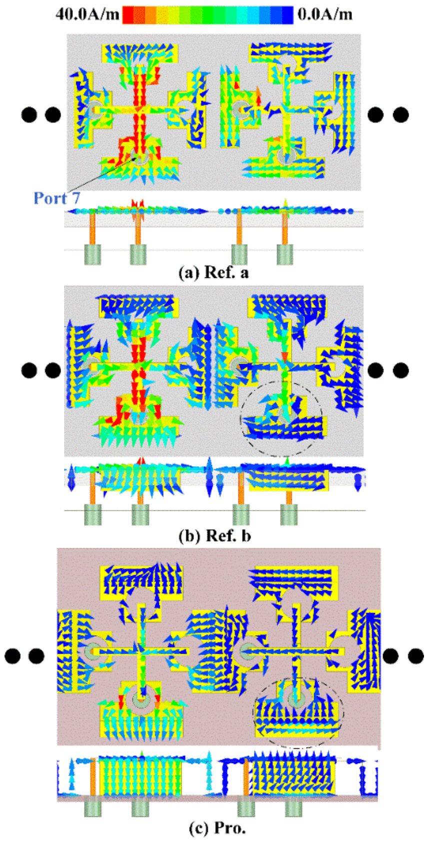


Fig. 13. Current distributions of three antenna arrays with exciting port 7.

*C. Scan performance of the linear array*

The simulated active reflection coefficients of the unit (the center unit) in the array at different scanning angles are shown in Fig. 14. It can be noted that the active $|S_{11}|$ is very well and always less than -10 dB in the operating bandwidth when the beam scans from 0° to 60° in the $x$-polarization. However, for the $y$-polarization, the active reflection coefficients are not well like the ones in Fig. 14 (a). They have a wide bandwidth and cover the proposed operation frequency band when the beam scans from 0° to 30°. But when the beam scans more than 30°, the frequency band shifts to higher frequency and the active $|S_{11}|$ is lower than -7.5 dB in the proposed operating frequency band.

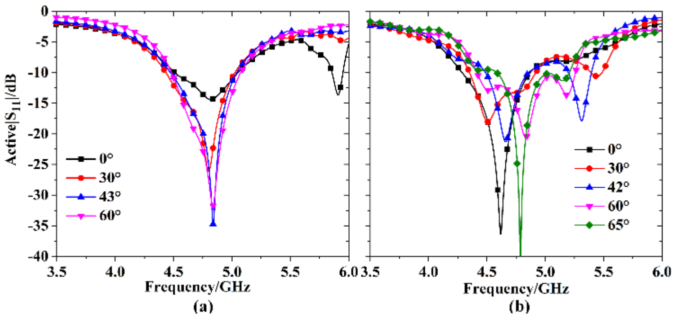


Fig. 14. Simulated active reflection coefficients of the units in the array and at different scanning angles: (a) port 7; (b) port 8.

The scanning performance of the proposed linear dual-polarization phased array at the middle frequency in the proposed operating bandwidth is reported in Fig. 15. For brevity, the scanning pattern at the middle frequency in the proposed operating bandwidth is descripted, but the scanning patterns at other frequencies including the side frequencies have similar scanning performance with the proposed results. For the $x$-polarization, it is important to note that the array can scan in the coverage of ±60°, meanwhile, the variation of the realized gain is less than 3 dB, and the gain of the scanning beam decreases with increasing the scanning angle. Besides, it can be found that the side-lobe level of each scanning beam is very low and lower than 9.5 dB without any optimization of excitation amplitude regardless of scanning to any angle. For the $y$-polarization, the scanning beam at the key scanning angles like ±30°, ±45°, ±60° is given to validate the perfect scanning performance without any scanning blindness. And the pattern of the proposed array has a scanning coverage of ±65°. The realized gain reduction of the scanning beam varies less than 3 dB in the proposed scanning range, but which is no regularity, unlike the variation of the $x$-polarization. This is because there is a little fluctuation in the unit pattern of this plane. It is the same as the patterns of the $x$-polarization, the side-lobe level is very low in the scanning coverage except for 65°.

The one-by-eight dual-polarization linear array antenna is fabricated according to the previous design requirements. To minimize the effects of the manufacturing process, the plastic studs and the dielectric substrate (PP) which is processed into a special shape are used to fix the antenna structure. Eight phased shifts and one 1-to-8 power splitter are used to excite each unit by providing the same amplitude and different phases, as shown in Fig. 16(a). They are connected with coaxial cables of the same length. A SATIMO near-field measurement system is used to measure the radiation patterns of the antenna as shown in Fig. 16(b). When the typical antenna unit is selected to measure the performance, the other antenna units connect to the matching load.

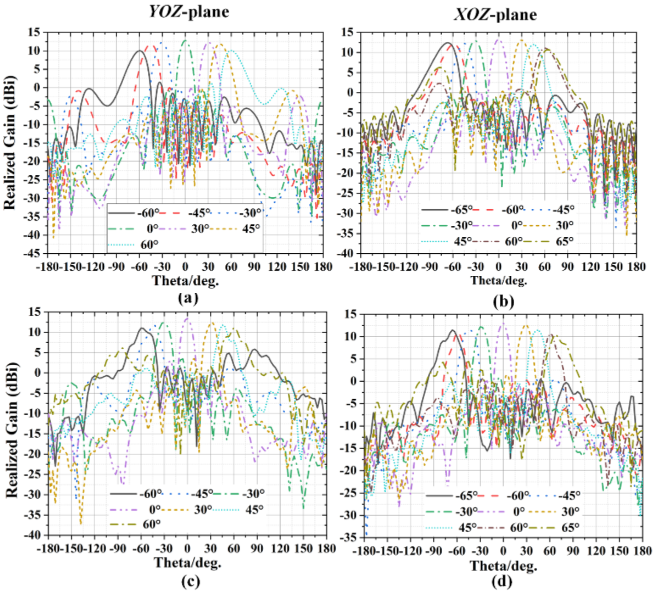


Fig. 15. Scanning radiation performance of the linear array antenna at 4.7 GHz; *x*-polarization: (a) simulation. and (c) measurement; *y*-polarization: (b) simulation and (d) measurement.

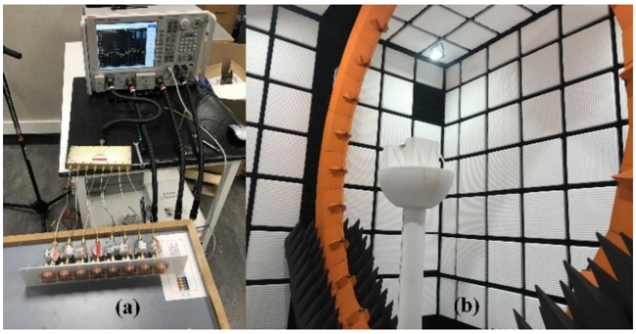


Fig. 16. Prototype of the proposed linear array and detailed illustration for measurement.

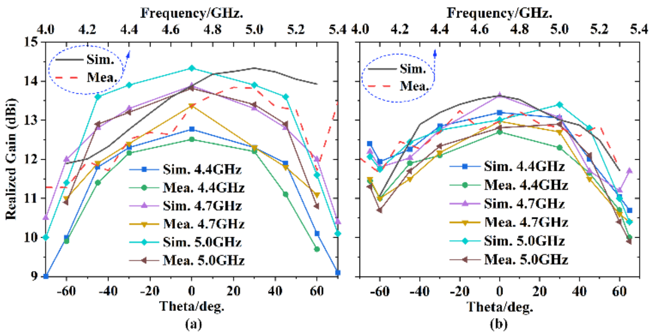


Fig. 17. Simulated and measured scanning realized gain of the linear array antenna at different frequencies with varying scanning angles: (a) *x*-polarization; (b) *y*-polarization.

The measured *S*-parameters of the proposed linear array are shown in Fig. 9. The measured results are very similar to the simulated results compared with the curves. Hence, the operating frequency band of the proposed linear array is from 4.35 to 5.15 GHz in *x*-polarization and 4.4 to 5.15 GHz in *y*-polarization, respectively. Meanwhile, the mutual coupling in the array for both polarizations is all better than -20 dB, and the measured port isolation is higher than 23 dB and better than the simulated results. The measured radiation pattern of the center antenna unit in the array is given in Fig. 11. By compared the simulations and measurements, they have a good agreement. But the curves of the pattern in the *y*-polarization have a little difference. The radiation performance in this plane is more sensitive, and the above difference is caused by manufacturing errors.

Measurements for the far-field scanning performance are reported in Fig. 15 (c) and (d). According to the situation of the simulation, the scanning results at the middle frequency is presented to validate the proposed scanning capability. Note that the proposed measurement demonstrates the array can scan in the coverage of ±60° in the *x*-polarization and in the coverage of ±65° in the *y*-polarization, respectively, meanwhile, the realized gain reduction in the scanning overage is lower than 3 dB, which is similar to the simulated results. However, the curves of the scanning patterns of the measurements have some differences from the ones of the simulations. This is because the phase shifter and the power splitter cause the input amplitude of each port to be different, but it doesn't affect the beam direction. Concurrently, the side-lobe level of the measured patterns has a little difference, which is lower than -7.5 dB. The detailed realized gain of the array in two polarizations is shown in Fig. 17. In the operating frequency band, the gain at the broadside direction of the *x*-polarization increases from 12.8 dBi to 14.4 dBi with shifting the frequency. But for the *y*-polarization, the gain variation with the frequency is from 13.0 to 13.5 dBi and its maximum at 4.7 GHz. The measured results are similar to the simulated ones but have a little difference. Additionally, the detailed gain variation with the scanning angle at different frequencies is also presented in Fig. 17. Note that the good scanning capability is realized in the proposed operating bandwidth.

## IV. The Dual-Polarization Planar Array

### A. Antenna design and analysis

TABLE III
DIMENSIONS OF THE ANTENNA UNIT OF PLANAR ANTENNA

| Parameter | $L_0$ | $L_1$ | $L_f$ | $W_1$ | $W_f$ | $r_0$ | $h_1$ | $h_2$ | $W_2$ |
|---|---|---|---|---|---|---|---|---|---|
| Units (mm) | 15.5 | 7.5 | 18.5 | 3.5 | 1.5 | 3 | 6.0 | 0.5 | 4.2 |

To demonstrate the effect of the proposed method for the dual-polarization planar array, a 4 × 8 planar phased array antenna is designed and fabricated as shown in Fig. 18. In *xoz*-plane, it is different from the linear array, which is connected to each unit cells by the metal sheet. Hence, the size of the proposed antenna unit has a little difference from the one in the linear array to ensure good impedance performance, where's given in Table III. But the other design of the planar array is completely in line with the requirements of the linear array in

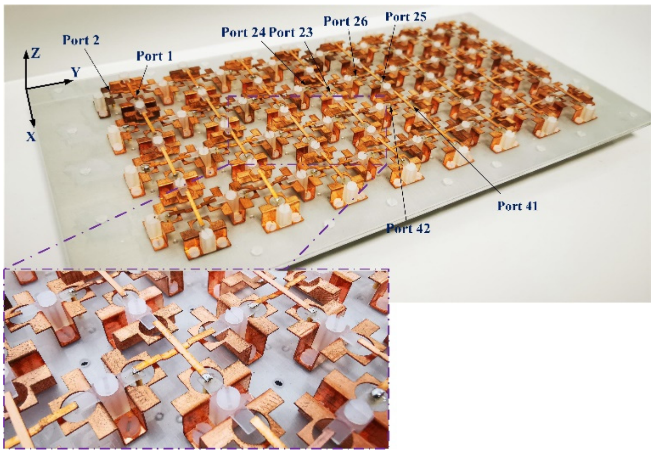

Fig. 18. The configuration of the planar array antenna.

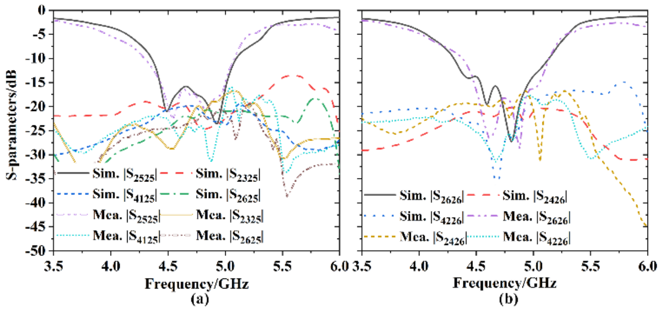

Fig. 19. Simulated and measured *S*-parameters of the units in the planar array: (a) *x*-polarization; (b) *y*-polarization.

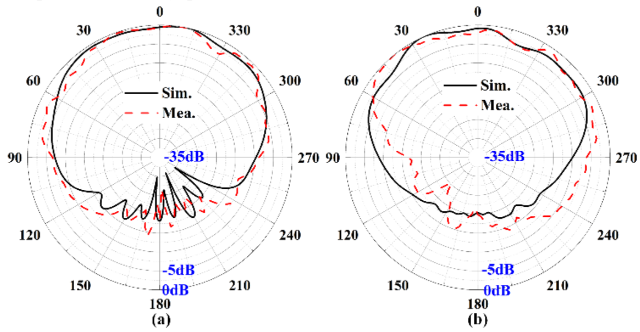

Fig. 20. Radiation patterns of the center unit in the proposed planar array in *yoz*-plane: (a)port 25; (b)port 26.

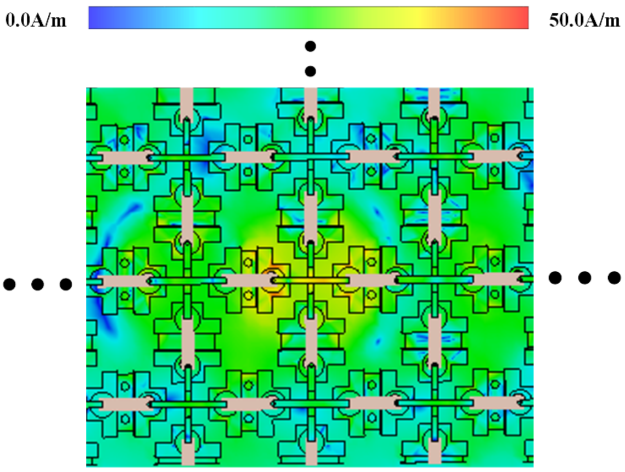

Fig. 21. Current distribution of the planar array antenna at 4.7 GHz.

substrate. The size of the planar ground is 150 mm× 290 mm, and large enough to exclude the impact on the wide-angle scanning performance of the array antenna.

As depicted in Fig. 19, the *S*-parameters of the planar array are presented. The proposed planar array can operate in the frequency band from 4.4 GHz to 5.0 GHz with dual-polarization. Similarly, the CCM is used to improve the performance of the planar array. The mutual coupling in the array is all better than -20 dB in the proposed operating frequency band except in the higher frequency band lower than -18 dB. Meanwhile, the port isolation of the unit in the array is also higher than 23 dB. For the detailed operating principle of the proposed method, it has been presented in the above section. In the same way, for verifying the effect of the proposed method on the radiation performance, the radiation patterns of the center unit in the proposed planar array are presented in Fig. 20. It is important to note that the patterns are the wide beam-width for two ports, respectively. Although there are some indentations in the curves of the patterns, this couldn't affect the unit's wide-beam characteristic. The reason for the above is similar to that of the linear array. To validate the proposed method in the planar array, the simulated current distribution of the planar array is shown in Fig. 21. The intense current just produces on the droved unit and hardly induces to the adjacent units. Because of the symmetrical structure, the proposed function also realized in another plane. Therefore, the current cancellation function is realized, which is the same as the analysis of the decoupling principle. Besides, the horizontal and vertical currents still are produced in the antenna unit to guarantee the wide beam-width performance.

### *B. Scanning performance*

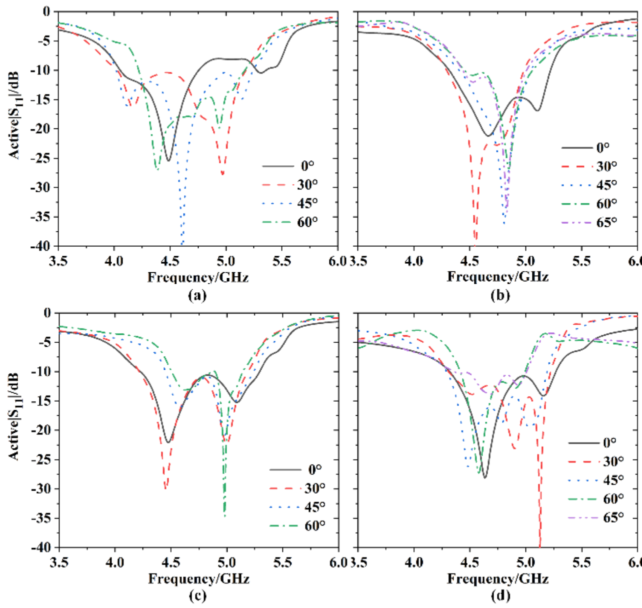

Fig. 22. Simulated active reflection coefficients of the units in the planar array at different scanning angles: (a)port 1; (b) port 2; (c) port 23; (d) port 24.

The simulated active reflection coefficients of the units in the proposed dual-polarization planar array at different scanning angles are shown in Fig. 22. The edge unit and center unit are chosen as two typical units to analyze the active impedance characteristic. It is observed that the active $|S_{11}|$ of the edge unit is less than -7.5 dB in the operating bandwidth regardless of scanning to any angle in the scanning coverage. For the center unit, the active impedance characteristic is relatively stable with varying the scanning angle and most active $|S_{11}|$ is lower than -10 dB. Besides, it can be noted that the active impedance bandwidth (≤ -10 dB) would change narrow with increasing the scanning angle. For the *y*-polarization, the unit can get a good impedance characteristic when the beam scans up to 65°, which has larger scanning coverage than the one in the *x*-polarization. In the same way, for verifying the function of the proposed method on the radiation performance, the radiation patterns of the center unit in the proposed planar array are presented in Fig. 23. It is important to note that the patterns are the wide beam-width of two ports, respectively. Although there are some indentations in the curves of the patterns, this does not affect the unit's wide-beam characteristic. The reason for the above is similar to that of the linear array. Therefore, the proposed method not only ensures the units in the planar array radiating a wide beam-width pattern, but also reduces the coupling of the array to improve the active impedance characteristic.

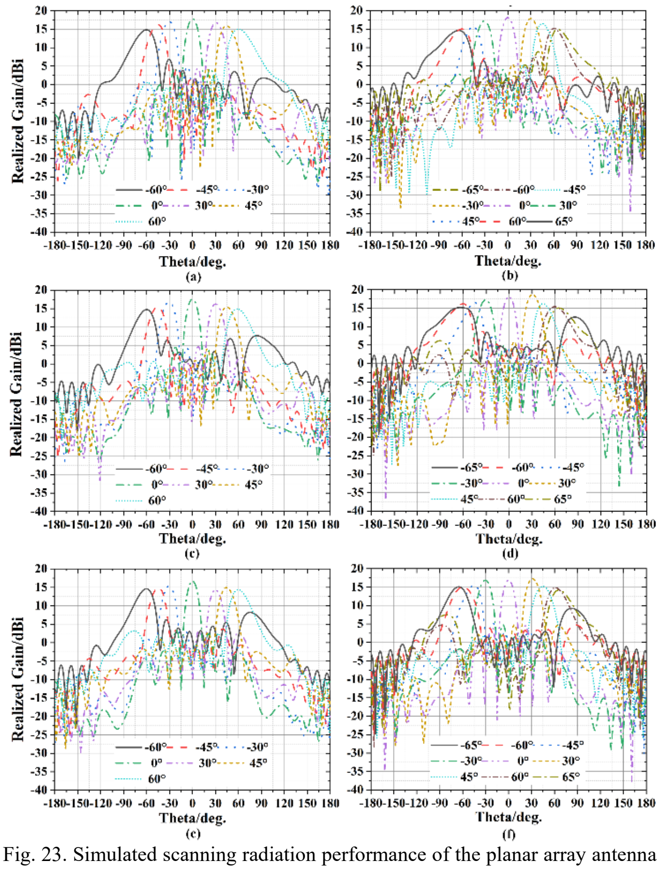


Fig. 23. Simulated scanning radiation performance of the planar array antenna at different frequencies in *yoz*-plane; *x*-polarization: (a) 4.4 GHz; (c) 4.7 GHz; (e) 5.0 GHz; *y*-polarization: (b) 4.4 GHz; (d) 4.7 GHz; (f) 5.0 GHz.

The above analysis has proved that the proposed dual-polarized planar array meets the requirements of achieving wide-angle scanning performance. Hence, the simulated scanning radiation patterns of the planar array with three typical frequencies (4.4 GHz, 4.7 GHz, 5.0 GHz) are reported in Fig. 23. For the *x*-polarization, the planar array has a large scanning coverage from -60° to 60°, and the scanning realized the gain reduction in the scanning coverage is less than 3 dB. And the gain drops with increasing the scanning angle. The side-lobe level is very low and lower than -10 dB except at -60°. For the *y*-polarization, the planar array can scan in the scanning coverage of ±65°, where's realized gain reduction is also lower than 3 dB. The gain variation of the scanning pattern is unregular because of the unit pattern fluctuation in the array. In the scanning coverage of ±60°, the side-lobe level of the patterns is very low and lower than -10 dB in the operating frequency band. The detailed realized gain with the variation of scanning angles at different frequencies is shown in Fig. 26. Compared with the scanning performance of the linear array, it is observed that most of the scanning performance is similar except for the side-lobe level when scanning up to 60°.

### C. *Measurements*

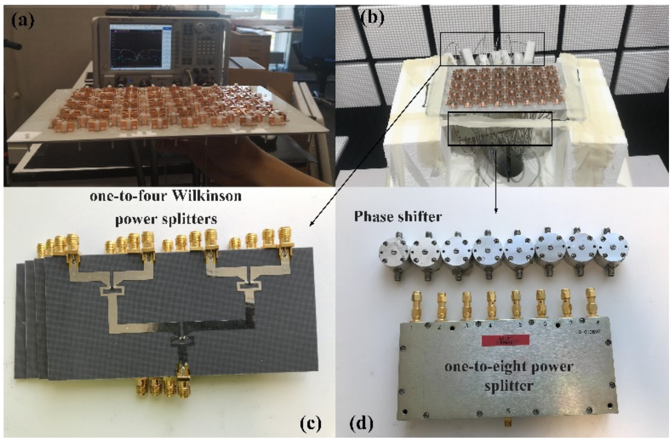


Fig. 24. Prototype of the proposed planar array and detailed illustration for measurement.

According to the design dimensions in Table III, the dual-polarization planar array antenna is fabricated, and the *S*-parameters of the proposed planar array are measured as shown in Fig. 24(a). The radiation patterns of the planar array are measured in the SATIMO near-field anechoic chamber at the Aalborg University. The measurement is the same as the linear array except for the radiation patterns. The eight 1-to-4 power dividers, as shown in Fig. 24(c), are applied to connect the eight phase shifters (as shown in Fig. 24(d)) and 32 ports of the antenna units for providing the same amplitude and different phases. And the other 32 ports of the antenna units connect to the matching load. The one-to-eight power splitter connects to the eight phase shifters and offers the input source for the above array. The measured *S*-parameters of the proposed planar array are shown in Fig. 19. And the measured results agree well with the simulated. The proposed dual-polarization planar array can operate in the frequency band from 4.4 GHz to 5.0 GHz, which's mutual coupling is all the better than -19 dB regardless of any ports. Meanwhile, the port isolation is also higher than 22 dB. The measured radiation pattern of the center antenna unit in the array is given in Fig. 20. By compared the simulations and measurements, they have a good agreement. But there is a little different mainly due to the manufacturing errors.

The measured scanning patterns of the proposed array are shown in Fig. 25. The analysis is similar to the simulated one, three different frequencies are selected to validate the

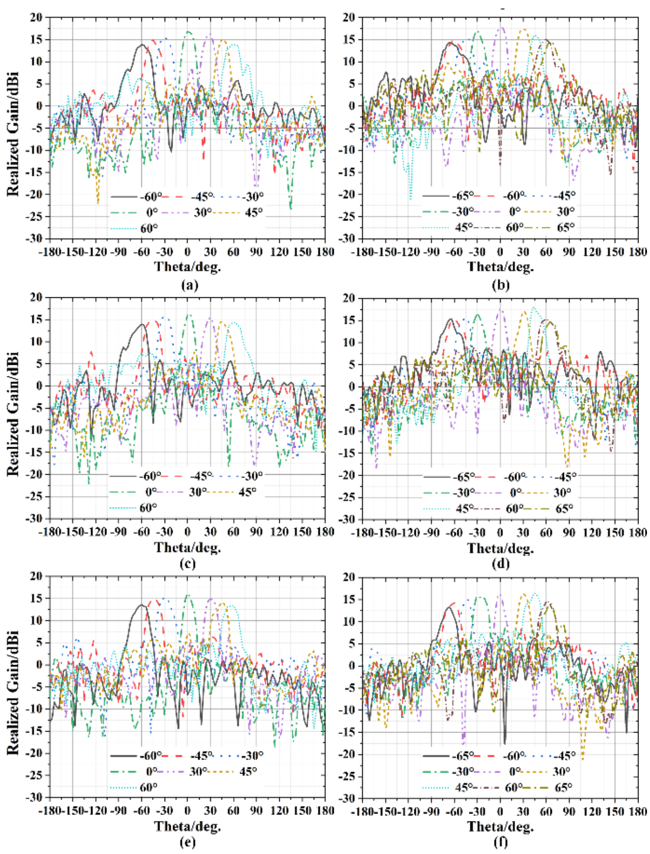

Fig. 25. Measured scanning radiation performance of the planar array antenna at different frequencies in *yoz*-plane; *x*-polarization: (a) 4.4 GHz; (c) 4.7 GHz; (e) 5.0 GHz; *y*-polarization: (b) 4.4 GHz; (d) 4.7 GHz; (f) 5.0 GHz.

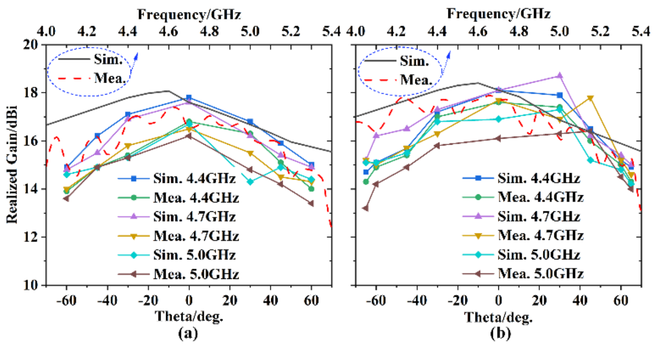

Fig. 26. Simulated and measured scanning realized gain of the planar array antenna at different frequencies with varying scanning angles in *yoz*-plane: (a) *x*-polarization; (b) *y*-polarization.

scanning performance in the whole operating frequency band. It can be found that the proposed dual-polarization array can scan in the coverage of ±60°and ±65° for two polarizations in *yoz*-plane, respectively, and the realized gain reduction in the scanning overage is lower than 3 dB, which are in agreement with the simulated results. However, the curves of the scanning patterns of the measurements have some differences with the ones of the simulations, especially at scanning up to large angles. The season is the same as the one in the linear array. The side-lobe level of the scanning patterns is lower than -8.0 dB. The detailed realized gain of the array is shown in Fig. 26. In the operating frequency band, it can be seen that the change trend of the gain is the same with shifting the frequency. And the gain variation is from 17.8 to 18.2 dBi. Besides, the measured gain is about 0.5 dB less than the simulated gain. In the scanning coverage, the gain fluctuation is less than 3 dB. The detailed gain variation with scanning angle at different frequencies is shown in Fig. 27. Therefore, the wide-angle scanning performance is verified and realized in *yoz*-plane of a new four-by-eight dual-polarized planar array by a simple and good method. Similarly, the scanning performance in *xoz*-plane of the planar array is also realized by the proposed method.

## V. Discussion

TABLE IV
COMPARISON OF DIFFERENT DUAL-POLARIZATION ANTENNAS

| Ref. | BW | Height (λ) | MC (dB) | SR (Deg.) | GF (dB) | ISO (dB) | SLL (dB) |
|---|---|---|---|---|---|---|---|
| [29] | 26.1% 2.0-2.6GHz | 0.06 | / | ±50°(linear) | 4.5 | <25 | / |
| [30] | 2.1% 5.2-5.3GHz | 0.03 | -16 | ±66°(planar) | 3.5 | <15 | <-5.4 |
| [31] | 16.1% 3.7-4.4GHz | 0.23 | / | ±45°(planar) | / | <25 | / |
| [32] | 31.1% 26-32 GHz | 0.29 | -11 | ±60°(planar) | / | <15 | / |
| [33] | 3.0% 4.9-5.1GHz | 0.08 | / | ±64°(planar) | 4.5 | / | <-9.3 |
| [34] | 66.7% 2.5-5.0GHz | 0.14 | -11 | ±45°(planar) | 3.3 | 7 | <-9.3 |
| **Pro.** | **12.8% 4.4-5.0GHz** | **0.11** | **-20 -19** | **±65°(linear) ±65°(planar)** | **3.0** | **<22** | **<-7.5 <-8.0** |

Note: MC: port-to-port mutual coupling of all the units. SR: scanning range. GF: gain fluctuation in the scanning range. ISO: the isolation of the dual-polarized ports in each unit. SLL: side-lobe level. λ is the wavelength at the center frequency in the bandwidth.

So far, many scholars around the world have done a lot of research work in this area. Table IV lists some representative achievements compared with our work. It can be noted that it has a wide band and low profile, but the scanning coverage is not very large, and the gain fluctuation is not well in [29]. In [30], the work has a large scanning coverage, but the bandwidth of the antenna is narrower, and the side-lobe level is higher. The antenna has a wide operating frequency band and higher port isolation in [31]. However, it has a higher profile and limited scanning coverage. The antenna in [32] has a good scanning performance, but its profile is higher, and the port isolation is also lower. In [33], this work has a wide scanning coverage and lower side-lobe level, but its bandwidth is narrower, and gain fluctuation is not well. In [34], the tightly coupling array is introduced, which has a wideband but high profile, high mutual coupling as well as low port isolation. The proposed work has a low profile, larger scanning coverage, a lower gain fluctuation, good port isolation and side-lobe level compared with the other works. Moreover, our design not only achieves the wide-angle scanning capability in the dual polarization array, but also contributes to improving the port-to-port mutual coupling between the units in the array. The MC in the proposed array is better to any other similar published work although some port isolation in each unit has been slightly sacrificed based on the best of our knowledge. Hence, the proposed antenna is very suitable for 5G communication systems.

## VI. Conclusion

A new dual-polarization antenna and the current cancellation method are presented to improve the wide-angle scanning performance for satisfying the requirements for 5G communication system in this paper. The new decoupling method is discussed and applied in the proposed array to improve the mutual coupling, where is realized by a simple structure in the array. Besides, the structure not only improves the coupling but also extends the beam-width of the antenna unit in the array and makes the structure compact. To corroborate the above decoupling method, a 1×8 dual-polarization linear array and a 4×8 dual-polarization planar array are designed and demonstrated, and they have a good wide-angle scanning impedance in the large scanning coverage. The antenna unit can radiate the wide-beam in the array. Therefore, the linear array and planar array in *yoz*-plane can scan in the coverage of ±60° in the *x*-polarization and in the coverage of ±65° in the *y*-polarization, respectively, meanwhile, the realized gain reduction in the scanning overage is lower than 3 dB. Furthermore, two array prototypes are fabricated and characterized, yielding good performance with overall operational bandwidth. The measured results have a good agreement with the simulated results. In summary, combined with a low-profile dual-polarization antenna unit, the decoupling method is applied to realize dual-polarization wide-angle scanning phased array, which is a good solution for 5G communication system.

## Acknowledgement

The authors would like thank Ben Klauman Krøyer, Kristian Bank, and Kim Olesen for his assistance during the antenna fabrication and measurements.

## References

[1] S. E. Valavan, D. Tran, A. G. Yarovoy, A. G. Roederer, "Planar Dual-Band Wide-Scan Phased Array in X-Band," *IEEE Trans. Antennas Propag.*, vol. 62, no. 10, pp. 5370-5375, Oct. 2014.

[2] R. Wang, B. Z. Wang, C. Hu, and X. Ding, "Wide-Angle Scanning Planar Array with Quasi-Hemispherical-Pattern Units," Scientific Reports, vol. 7, no. 1, pp. 2729, Jun. 2017.

[3] G. Yang, J. Li, S. G. Zhou, Y. Qi. "A Wide-Angle Scanning E-plane Linear Array Antenna with Wide Beam Elements," *IEEE Antennas Wireless Propag. Lett.*, vol. 16, pp. 2923–2926, Oct. 2017.

[4] A. Kedar and K. S. Beenamole. "Wide Beam Tapered Slot Antenna for Wide-angle Scanning Phased Array Antenna," Progress In Electromagnetics Research B, vol. 08, no. 1, pp. 235-251, 2011.

[5] Y. Q. Wen, B. Z. Wang, X. Ding, "Wide-Beam Siw-Slot Antenna for Wide-Angle Scanning Phased Array," *IEEE Antennas Wireless Propag. Lett.*, vol. 15, pp. 1638-1641, 2016.

[6] E. G. Magil, H. A. Wheeler, "Wide-Angle Impedance Matching of A Planar Array Antenna by A Dielectric Sheet," *IEEE Trans. Antennas Propag.*, vol. 14, no. 1, pp. 49-53, 1966.

[7] P. Munk, "On Arrays that Maintain Superior CP and Constant Scan Impedance for Large Scan Angles," *IEEE Trans. Antennas Propag.*, vol. 51, no. 2, pp. 322-330, Apr. 2003.

[8] M. N. M. Kehn, L. Shafai, "Improved Matching of Waveguide Focal Plane Arrays Using Patch Array Covers as Compared to Conventional Dielectric Sheets," *IEEE Trans. Antennas Propag.*, vol. 57, no. 10, pp. 3062-3076, Jul. 2009.

[9] L. Gu, Y. W. Zhao, Q. M. Cai, Z. P. Zhang, B. H. Xu, Z. P. Nie, "Scanning Enhanced Low-profile Broadband Phased Array with Radiator-sharing Approach and Defected Ground Structures," *IEEE Trans. Antennas Propag.*, vol. 65, no. 11, pp. 5846-5854, Nov. 2017.

[10] F. Caminita, S. Costanzo, G. D. Massa, G. Guarnieri, S. Maci, G. Mauriello, I. Venneri, "Reduction of Patch Antenna Coupling by Using a Compact EBG Formed by Shorted Strips with Interlocked Branch-Stubs," *IEEE Antennas Wireless Propag. Lett.*, vol. 8, pp. 811-814, Apr. 2009.

[11] M. Li, S. Q. Xiao, B. Z. Wang. "Investigation of Using High Impedance Surfaces for Wide-Angle Scanning Arrays," *IEEE Trans. Antennas Propag.*, vol. 63, no. 7, pp. 2895-2901, Apr. 2015.

[12] G. Yang, J. Li, R. Xu, Y. M. Y. Qi, "Improving the Performance of Wide-Angle Scanning Antenna Array with High Impedance Periodic Structure," *IEEE Antennas Wireless Propag. Lett.*, vol. 15, pp. 1819–1822, Mar. 2016.

[13] R. L. Xia, S. W. Qu, P. F. Li, D. Q. Yang, S. Yang, Z. P. Nie, "Wide-Angle Scanning Phased Array Using an Efficient Decoupling Network," *IEEE Trans. Antennas Propag.*, vol. 63, no. 11, pp. 5161-5165, Sep. 2015.

[14] J. A. Kasemodel, C. C. Chen, J. L. Volakis, "Wideband planar array with integrated feed and matching network for wide-angle scanning," *IEEE Trans. Antennas Propag.*, vol. 61, no. 9, pp. 4528-4537, Jun. 2013.

[15] B. A. Arand, A. Bazrkar, A. Zahedi, "Design of a Phased Array in Triangular Grid with an Efficient Matching Network and Reduced Mutual Coupling for Wide-Angle Scanning," *IEEE Trans. Antennas Propag.*, vol. 65, no. 6, pp. 2983-2991, Jun. 2017.

[16] M. H. Awida, A. H. Kamel, A. E. Fathy, "Analysis and Design of Wide-Scan Angle Wide-Band Phased Arrays of Substrate-Integrated Cavity-Backed Patches," *IEEE Trans. Antennas Propag.*, vol. 61, no. 6, pp. 3034-3041, Jun. 2013.

[17] R. Lian, Z. Wang, Y. Yin, J. Wu and X. Song, "Design of a Low-Profile Dual-Polarized Stepped Slot Antenna Array for Base Station," *IEEE Antennas Wireless Propag. Lett.*, vol. 15, pp. 362-365, 2016.

[18] Y. He, Z. Pan, X. Cheng, Y. He, J. Qiao and M. M. Tentzeris, "A Novel Dual-Band, Dual-Polarized, Miniaturized and Low-Profile Base Station Antenna," *IEEE Trans. Antennas Propag.*, vol. 63, no. 12, pp. 5399-5408, Dec. 2015.

[19] Q. Zhang and Y. Gao, "A Compact Broadband Dual-Polarized Antenna Array for Base Stations," *IEEE Antennas Wireless Propag. Lett.*, vol. 17, no. 6, pp. 1073-1076, June 2018.

[20] K. Wang, X. Liang, W. Zhu, et al., "A Dual-Wideband Dual-Polarized Aperture-Shared Patch Antenna with High Isolation," *IEEE Antennas Wireless Propag. Lett.*, vol. 17, no. 5, pp. 735-738, May 2018.

[21] R. C. Paryani, P. F. Wahid and N. Behdad, "A Wideband, Dual-Polarized, Substrate-Integrated Cavity-Backed Slot Antenna," *IEEE Antennas Wireless Propag. Lett.*, vol. 9, pp. 645-648, 2010.

[22] H. Li, L. Kang, F. Wei, Y. Cai and Y. Yin, "A Low-Profile Dual-Polarized Microstrip Antenna Array for Dual-Mode OAM Applications," *IEEE Antennas Wireless Propag. Lett.*, vol. 16, pp. 3022-3025, 2017.

[23] L. Ge and K.-M. Luk, "A low-profile magneto-electric dipole antenna," IEEE Trans. Antennas Propag., vol. 60, no. 4, pp. 1684–1689, Apr. 2012

[24] Q. Xue, S. W. Liao, and J. H. Xu, "A differentially-driven dual polarized magneto-electric dipole antenna," *IEEE Trans. Antennas Propag.*, vol. 61, no. 1, pp. 425–430, Jan. 2013.

[25] Z. L. Ma and C. H. Chan, "Waveguide-based differentially fed dual polarized magnetoelectric dipole antennas," *IEEE Trans. Antennas Propag.*, vol. 65, no. 8, pp. 3849–3857, Aug. 2017.

[26] Y. X. Sun and K. W. Leung, "Dual-band and wideband dual-polarized cylindrical dielectric resonator antennas," *IEEE Antennas Wireless Propag. Lett.*, vol. 12, pp. 384–387, 2013.

[27] H. Tang, J.-X. Chen, W.-W. Yang, L.-H. Zhou, and W. Li, "Differential dual-band dual-polarized dielectric resonator antenna," *IEEE Trans. Antennas Propag.*, vol. 65, no. 2, pp. 855–860, Feb. 2017.

[28] Z. Zhang and K. Wu, "A Wideband Dual-Polarized Dielectric Magnetoelectric Dipole Antenna," *IEEE Trans. Antennas Propag.*, vol. 66, no. 10, pp. 5590-5595, Oct. 2018.

[29] H. Wu, J. Geng, K. Wang, et al., "A Low-Profile Wideband Dual-Polarized Antenna Based on an Improved HIS and Its Broad-Angle Beam-Scanning Array," *IEEE Antennas Wireless Propag. Lett.*, vol. 19, no. 3, pp. 383-387, March 2020.

[30] Y. Wen, S. Gao, B. Wang and Q. Luo, "Dual-Polarized and Wide-Angle Scanning Microstrip Phased Array," *IEEE Trans. Antennas Propag.*, vol. 66, no. 7, pp. 3775-3780, July 2018.

[31] P. Zhang, S. Qu and S. Yang, "Dual-Polarized Planar Phased Array Antenna with Cavity-Backed Elements," *IEEE Antennas Wireless Propag. Lett.*, vol. 18, no. 9, pp. 1736-1740, Sept. 2019.

[32] T. Chaloun, V. Ziegler and W. Menzel, "Design of a Dual-Polarized Stacked Patch Antenna for Wide-Angle Scanning Reflectarrays," *IEEE Trans. Antennas Propag.*, vol. 64, no. 8, pp. 3380-3390, Aug. 2016.

[33] G. Gao, X. Ding, Y. Cheng and W. Shao, “Dual-Polarized Wide-Angle Scanning Phased Array Based on Mutimode Patch Elements,” *IEEE Antennas Wireless Propag. Lett.*, vol. 18, no. 3, pp. 546-550, March 2019.
[34] Q. Chen, Z. Li, W. Wang, Z. Huang, X. Liang and X. Wu, “A Broadband Dual-polarized Solar Cell Phased Array Antenna,” *IEEE Trans. Antennas Propag.*, doi: 10.1109/TAP.2021.3098520.
[35] H. Zhang, S. Yang, Y. Chen, J. Guo and Z. Nie, “Wideband Dual-Polarized Linear Array of Tightly Coupled Elements,” *IEEE Trans. Antennas Propag.*, vol. 66, no. 1, pp. 476-480, Jan. 2018.
[36] R. J. Bolt et al., “Characterization of a Dual-Polarized Connected-Dipole Array for Ku-Band Mobile Terminals,” *IEEE Trans. Antennas Propag.*, vol. 64, no. 2, pp. 591-598, Feb. 2016.
[37] S.-W. Su, C.-T. Lee, and F.-S. Chang, “Printed MIMO-antenna system using neutralization-line technique for wireless USB-dongle applications,” *IEEE Trans. Antennas Propag.*, vol. 60, no. 2, pp. 456–463, Feb. 2012.
[38] S. Zhang and G. F. Pedersen, “Mutual Coupling Reduction for UWB MIMO Antennas with a Wideband Neutralization Line,” *IEEE Antennas Wireless Propag. Lett.*, vol. 15, pp. 166-169, May 2016.
[39] G. -W. Yang and S. Zhang, “A Dual-Band Shared-Aperture Antenna with Wide-Angle Scanning Capability for Mobile System Applications,” IEEE Transactions on Vehicular Technology, vol. 70, no. 5, pp. 4088-4097, May 2021.
[40] Y. -M. Zhang and S. Zhang, “A Novel Aperture-Loaded Decoupling Concept for Patch Antenna Arrays,” IEEE Transactions on Microwave Theory and Techniques, vol. 69, no. 9, pp. 4272-4283, Sept. 2021.
[41] Y. -M. Zhang and S. Zhang, “A Decoupling and Matching Network with Harmonic Suppression for MIMO Antennas,” 15th European Conference on Antennas and Propagation (EuCAP), 2021, pp. 1-4.
[42] G. Yang, J. Li, J. Yang, S. G. Zhou. “A Wide Beamwidth and Wideband Magnetoelectric Dipole Antenna,” *IEEE Trans. Antennas Propag.*, vol. 66, no. 12, pp.6724-6733, Dec. 2018.
[43] H. Huang, Y. Liu and S. Gong, “A Broadband Dual-Polarized Base Station Antenna with Sturdy Construction," IEEE Antennas and Wireless Propagation Letters, vol. 16, pp. 665-668, 2017.
[44] N. Luo, Y. He, L. Zhang, S. -W. Wong, C. Li and Y. Huang, “A Differential Broadband Dual-Polarized Base Station Antenna Element for 4G And 5G Applications,” 2019 Computing, Communications and IoT Applications (ComComAp), 2019, pp. 337-340.
[45] Y. He, Z. Pan, X. Cheng, Y. He, J. Qiao and MM Tentzeris, “A Novel Dual-Band, Dual-Polarized, Miniaturized and Low-Profile Base Station Antenna,” IEEE Transactions on Antennas and Propagation, vol. 63, no. 12, pp. 5399-5408, Dec. 2015.

**Guang-Wei Yang (S’15-M’19)** received the B.E., M.S., and PhD. Degrees all in Electronic Engineering in Northwestern Polytechnial University in 2012, 2015, 2019, respectively. He is currently working at Queen Mary University of London as a Royal Society-Newton International Fellow. He was a Postdoc in the Antenna, Propagation and Millimeter-wave Systems (APMS) Section, Aalborg University, Denmark from 2019 to 2020. He also serves as a reviewer for all the IEEE and IET journals related to antennas. His recent research interests include wide beam antennas, wideband antennas, millimeter-wave array antennas, circularly-polarized antennas, base station antennas, 5G communication, phased array antennas, reconfigurable antennas, wide-angle scanning antenna Lens antennas, and microwave and optical metamaterials.

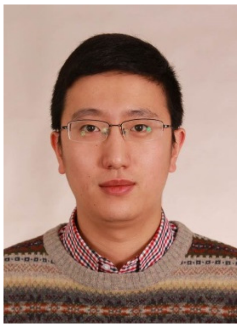

**Shuai Zhang (SM’18)** received the B.E. degree from the University of Electronic Science and Technology of China, Chengdu, China, in 2007 and the Ph.D. degree in electromagnetic engineering from the Royal Institute of Technology (KTH), Stockholm, Sweden, in 2013. After his Ph.D. studies, he was a Research Fellow at KTH. In April 2014, he joined Aalborg University, Denmark, where he currently works as Associate Professor and the leader of antennas group. In 2010 and 2011, he was a Visiting Researcher at Lund University, Sweden and at Sony Mobile Communications AB, Sweden, respectively. He was also an external antenna specialist at Bang & Olufsen, Denmark from 2016-2017. He has coauthored over 90 articles in well-reputed international journals and over 16 (US or WO) patents. His current research interests include: mmwave antennas for cellular communications, biological effects, metasurfaces, CubeSat antennas, Massive MIMO antennas, wireless sensors, and RFID antennas.